N87-22779

NONLINEAR HEAT TRANSFER AND STRUCTURAL ANALYSES OF SSME TURBINE BLADES

A. Abdul-Aziz
Sverdrup Technology, Inc.
Middleberg Heights, Ohio

and

A. Kaufman (Retired)
NASA Lewis Research Center
Cleveland, Ohio

Three-dimensional nonlinear finite-element heat transfer and structural analyses were performed for the first stage high-pressure fuel turbopump blade of the space shuttle main engine (SSME). Directionally solidified (DS) MAR-M 246 material properties were considered for the analyses. Analytical conditions were based on a typical test stand engine cycle. Blade temperature and stress-strain histories were calculated using MARC finite-element computer code (ref. 1). This study was undertaken to assess the structural response of an SSME turbine blade and to gain greater understanding of blade damage mechanisms, convective cooling effects, and the thermal-mechanical effects.

Hot-gas path components for reusable space propulsion systems operate under extreme gas pressure and temperature. These operating conditions subject the high pressure stage turbine nozzles and blades to severe thermal transients that can result in large inelastic strains and rapid crack initiation. Advances in casting techniques have allowed the development of directionally solidified and single crystal alloys for high temperature components in space propulsion vehicles. Mechanical anisotropy exhibited by these alloys have to be taken into account in the analytical studies. To improve the durability and accuracy of turbine blades and other hot section components, an accurate knowledge of the temperature and stress-strain histories at the critical location for crack initiation is required (fig. 1).

Experimental measurements of gas temperature profiles in the SSME turbopumps are difficult to obtain because of the high gas temperature and severe thermal transients. Turbine blade temperatures are primarily a function of hot gas flow and cooling. The temperature field is determined by the heat transfer from the hot gas to the blade. This heat transfer and its variations are determined by knowledge of the gas film coefficients. Also, the time-temperature history profile at the start transient, steady state, and cutoff is obtained through a combination of analytical and experimental results which is due to the complex flow phenomena through an accelerating turbine.

Temperature-dependent properties for the MAR-M 246 + Hf alloy were mainly provided by Rockwell International Corporation. These elastic properties are summarized in table I. Mean thermal coefficient of expansion data were converted to instantaneous values for MARC input. Longitudinal stress-strain properties, summarized in table II, were used for elastic-plastic region. The mission used for this analysis is shown in figures 2 and 3 in terms of inlet temperature, gas pressure, and revolutions per minute (RPM). This cycle is

applicable to a factory test of the engine; it is also reasonably representative of a flight mission except for the foreshortened steady-state operating time. The major factor inducing fatigue cracking is the transient thermal stresses caused by the sharp ignition and shutoff transients. The finite-element model of the blade in figure 4 was constructed of a three-dimensional eight-node isoparametric brick element. The model consisted of 1-25 elements with 1575 nodes and 4660 unsuppressed degrees of freedom.

Heat transfer coefficients at the blade airfoil (figs. 5(a) and (b)) were predicted by running a boundary layer analysis using a modified version of the STAN5 boundary layer code (refs. 2 and 3). Thermal environment experienced by the platform and shank were obtained from reference 4. Details regarding prediction of heat transfer coefficients at the stagnation region for the airfoil are available in reference 5. Transient results were obtained by scaling steady-state heat transfer coefficients based on transient flow and temperature. Predicted high temperature locations were evaluated for the two temperature spikes shown in figure 2.

The thermal response predicted from the finite-element analysis showed that the leading and trailing edges of the airfoil base are the hottest locations. Temperature distributions showed a cordwise variation at the first ignition spike and a spanwise variation thereafter into the cycle. A uniform temperature distribution was dominant at most of the airfoil surface during cruise except near the base at the platform junction where a mixture of cold and hot gas is present. The coldest spot was always at the blade root because of cooler boundary conditions. Blade temperature is shown in figures 6 through 8.

Elastic-plastic analyses have been conducted for the HPFTB blade with MARC code. Plastic strain calculations were based on incremental plasticity theory using Von Mises Yield criterion, the normality rule and a kinematic hardening model. The material elastic-plastic behavior was specified by the yield strengths and work hardening properties in the longitudinal direction; transverse properties were not available. Creep analyses were not performed at the present time because of inadequate knowledge of the creep characteristics for anisotropic blade material.

Incremental loading included centrifugal and gas pressure loads and metal temperature distributions as calculated from the heat transfer analysis. The same increments were used for the heat transfer and the elastic-plastic structural analysis. Approximately two million words of core storage on the CRAY-XMP computer were needed to run the problem. Analysis required about 4 hours of central processor unit (CPU) time on the CRAY system. The directionality of the elastic material properties causes anisotropic constraints. Lekhnitskii (ref. 6) has derived the generalized elastic strain equations for an anisotropic body with a transverse plane of isotropy. This anisotropic stress-strain law was incorporated in MARC user subroutine HOOKLW.

The colder airfoil base temperatures induce tensile thermal stresses at the critical leading edge location that are additive to the centrifugal stresses. A noticeable discrepancy is seen in the compressive strain region where the reduction in elastic analysis points resulted in failure to capture some of the cycle fluctuation due to transient thermal effects during the rapid engine cooldown. The CPU time for the elastic finite-element analyses amounted to 5 percent of that required for one cycle of the nonlinear finite-element

analysis. The critical location for crack initiation is at the leading edge near the base. Results of both elastic and inelastic structural analyses indicated the region of the finite-element model with the largest total strain range was coincident with the observed crack initiation site.

Radial stress distributions as calculated at the gaussian integration points closest to the suction and pressure surfaces are presented in figures 9 through 11. The stresses primarily reflect the centrifugal and thermal loadings. It is apparent that the analysis would not show a low-cycle fatigue problem if transient thermal effects were not considered.

REFERENCES

1. MARC General Purpose Finite Element Analysis Program. Vol. A: User Information Manual; vol. B: MARC Element Library. MARC Analysis Research Corporation, 1980.

2. Crawford, M.E.; and Kays, W.M.: STAN5 - A Program for Numerical Computation of Two-Dimensional Internal and External Boundary Layer Flows. NASA CR-2742, 1976.

3. Gaugler, R.E.: Some Modification to, and Operational Experiences With, The Two-Dimensional, Finite-Difference, Boundary-Layer Code, STAN5. NASA TM-81631, 1981. (Also, ASME Paper 81-GT-89, Mar. 1981.)

4. Space Shuttle Main Engine, Powerhead Structural Modeling, Stress and Fatigue Life Analysis. (LMSC-HREC-TR-D867333-1, Lockheed Missiles and Space Company; NASA Contract NAS8-34978) NASA CR-170999, 1983.

5. Abdul-Aziz, A.; Tong, M.; and Kaufman, K.: Thermal Finite-Element Analysis of an SSME Turbine Blade. Submitted for Presentation at the 1987 ASME/AIChE National Heat Transfer Conference, on Aug. 9-12, Pittsburgh, PA.

6. Lekhnitskii, S.G.; and Brandstatter, J.J., eds.: Theory of Elasticity of an Anisotropic Elastic Body. Holden-Day, Inc., 1963., pp. 24-25.

TABLE I. - DS MAR-M 246 PHYSICAL PROPERTIES

Temperature, °C	Modulus of elasticity, GPa		Means coefficient of thermal expansion, percent/°C
	Longitudinal	Transverse	
21	131	183	-------
93	120	179	0.00113
204	125	175	.00130
316	124	173	.00133
427	119	166	.00141
538	114	162	.00148
649	109	156	.00149
760	103	149	.00156
671	97	142	.00160

TABLE II. - DS MAR-M 246 STRESS-STRAIN PROPERTIES (LONGITUDINAL)

Plastic strain, percent	Stress, MPa		
	21 °C	649 °C	816 °C
0.1	800	808	875
.2	830	855	930
.4	850	895	965
.6	855	930	970
.8	865	945	975
1.0	870	960	980

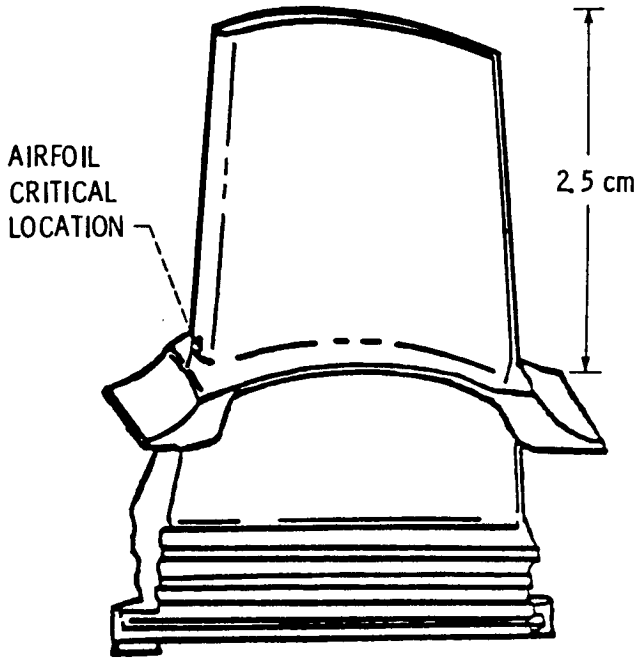

Figure 1. - SSME high-pressure fuel turbopump first stage turbine blade.

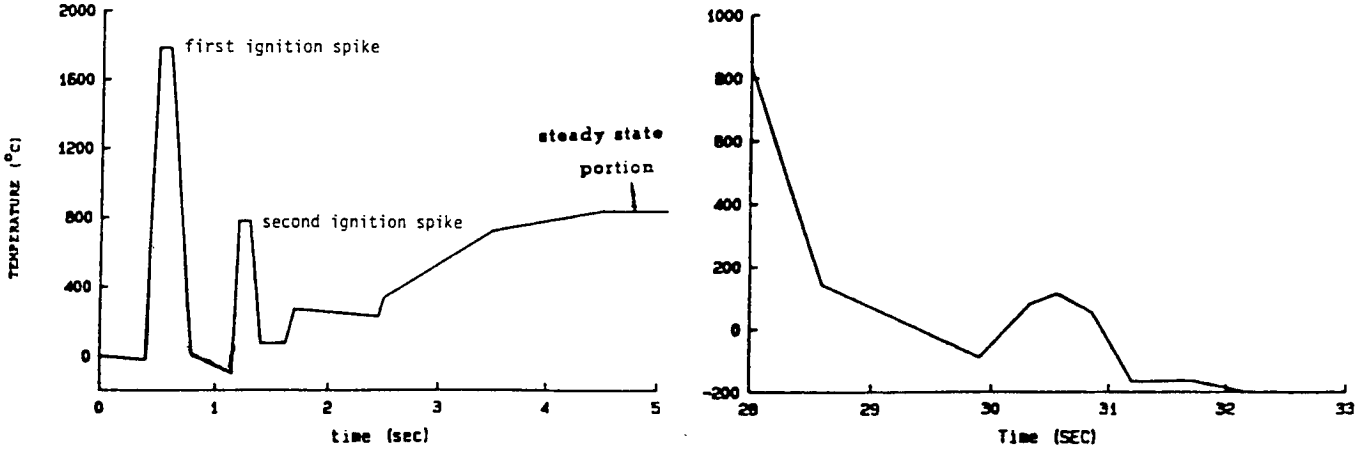

(a) Startup transient.

(b) Cutoff transient.

Figure 2. - Turbine inlet gas temperature for HPFTP.

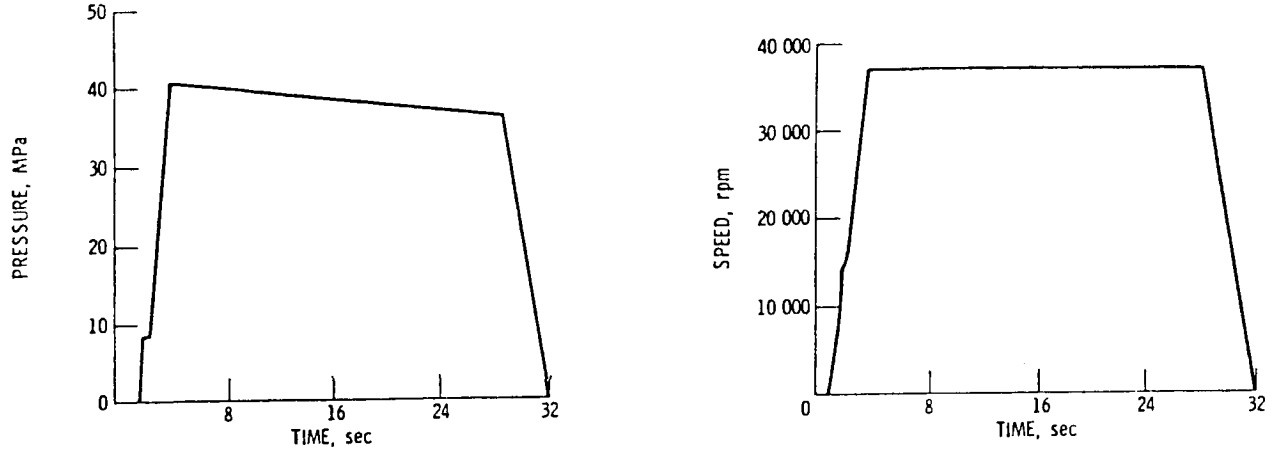

(a) Turbine inlet pressure.

(b) Blade rotational speed.

Figure 3. - Mission cycle used for analysis.

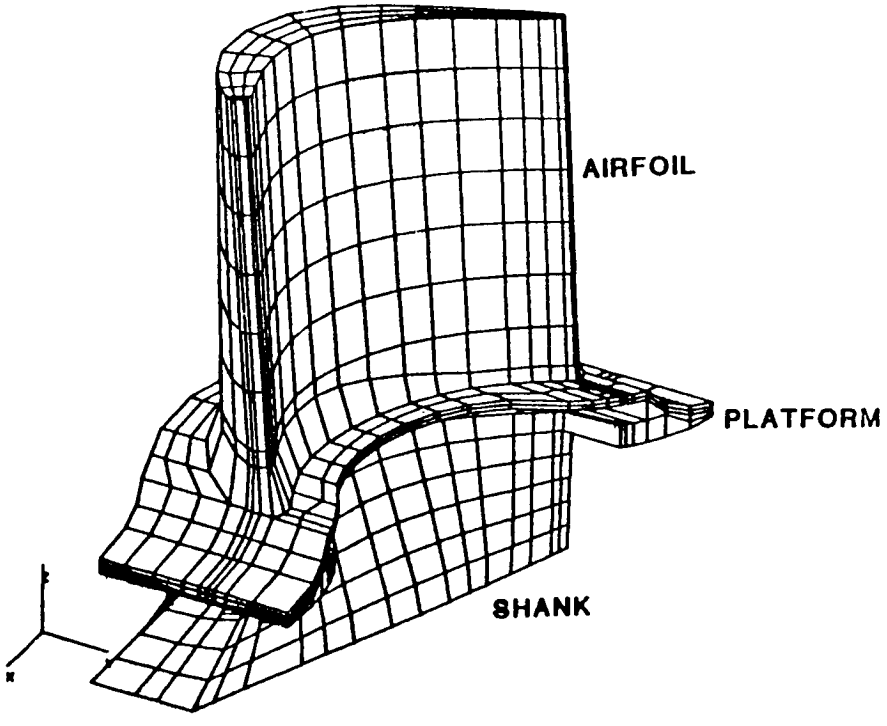

Figure 4. - HPFTP first-stage turbine blade MARC Model. (1575 nodes, 1025 elements)

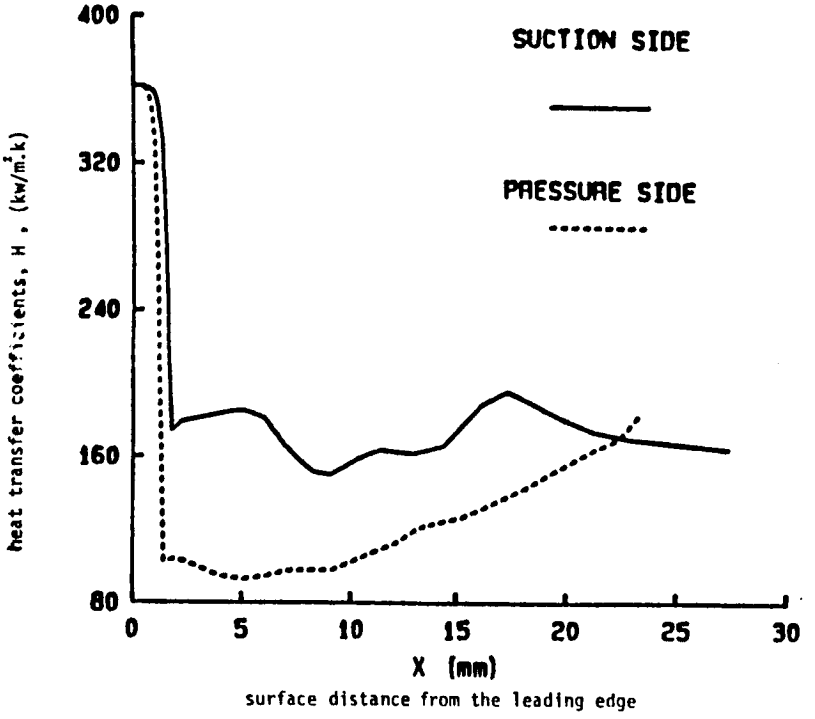

(a) At airfoil root.

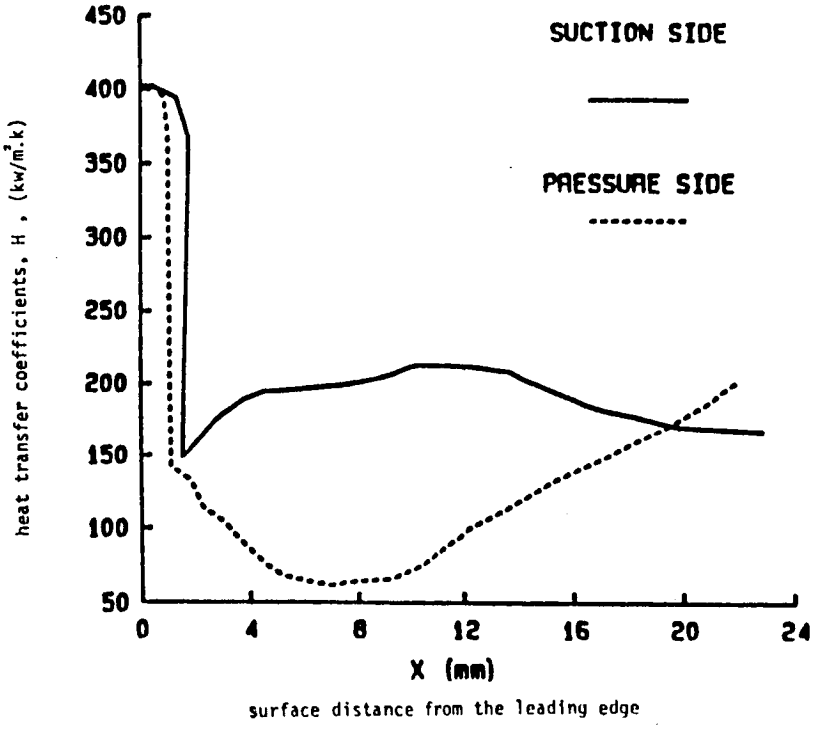

(b) At airfoil tip.

Figure 5. - Distribution of heat transfer coefficients.

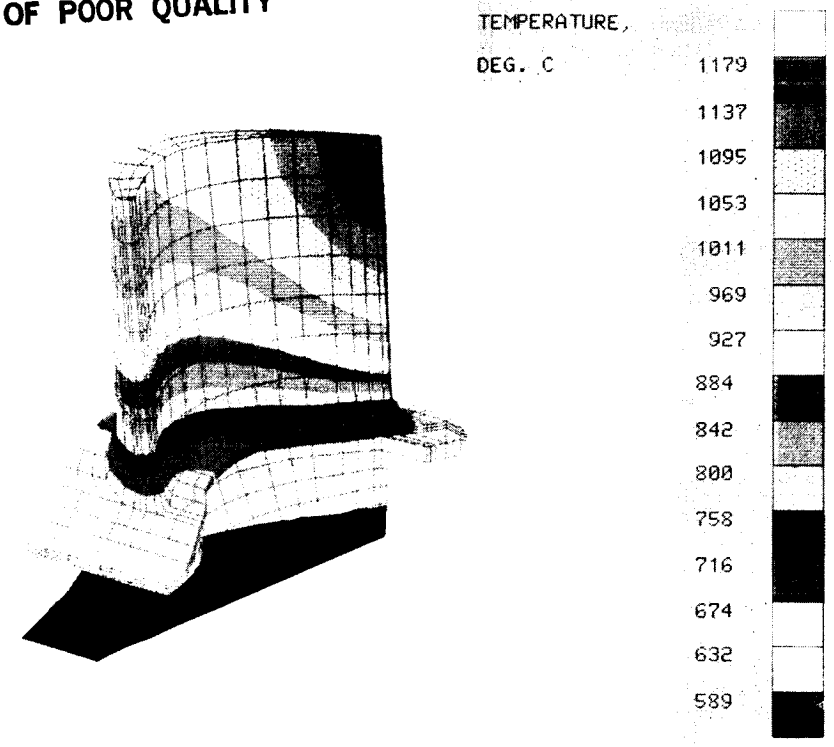

Figure 6. - Temperature contours at first ignition spike.

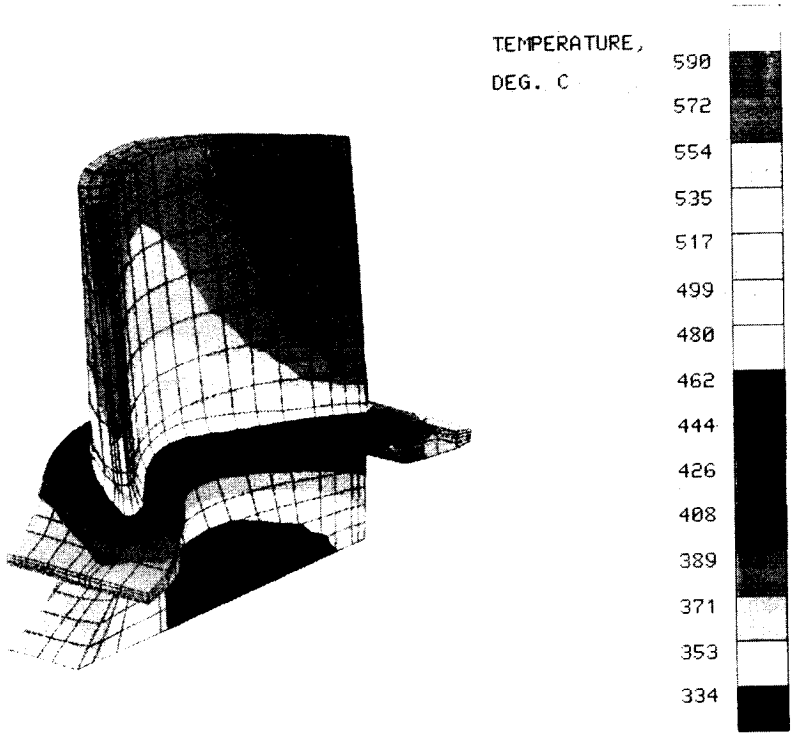

Figure 7. - Temperature at second ignition spike.

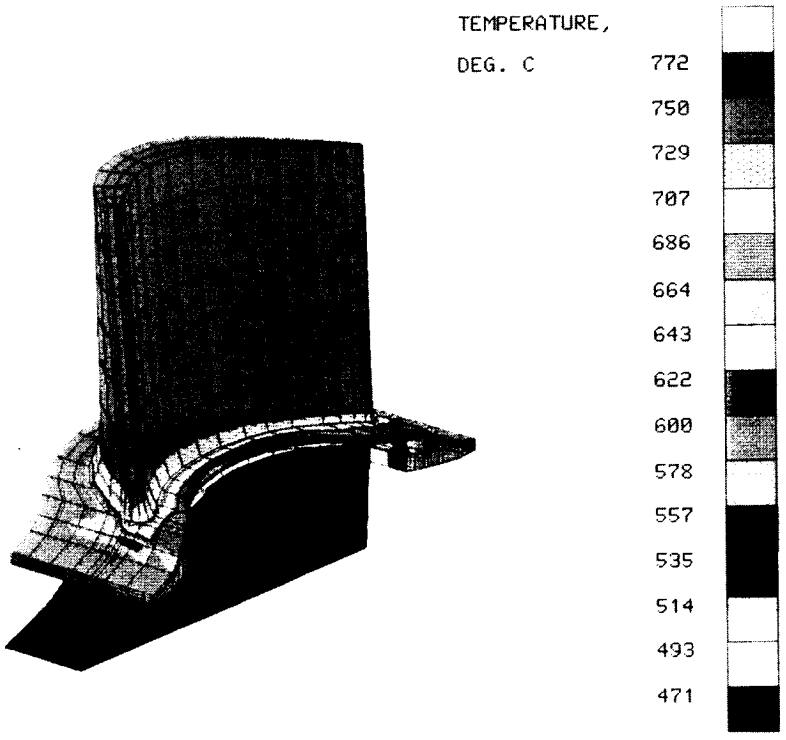

Figure 8. - Temperature contours during cruise.

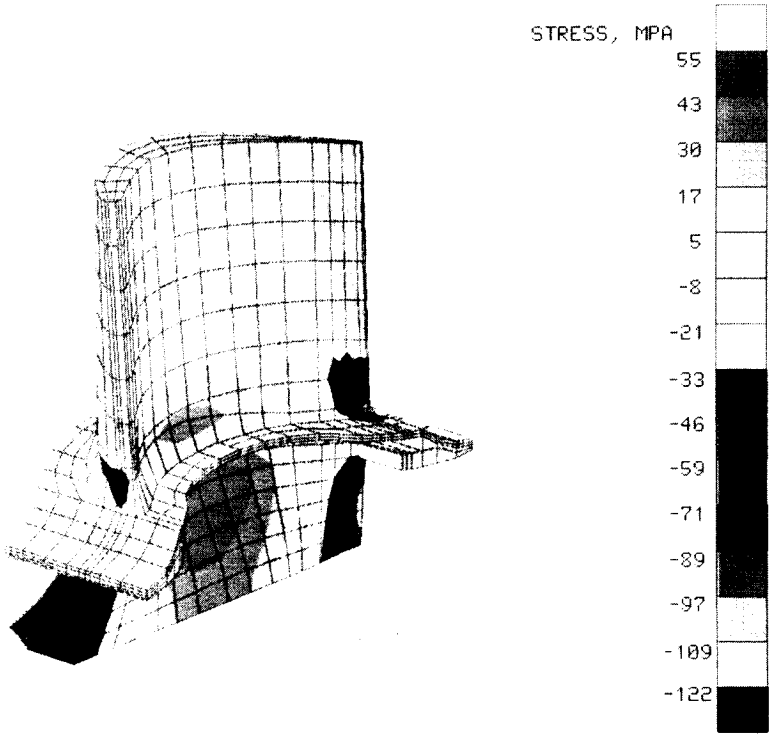

Figure 9. - Radial stresses at first ignition spike.

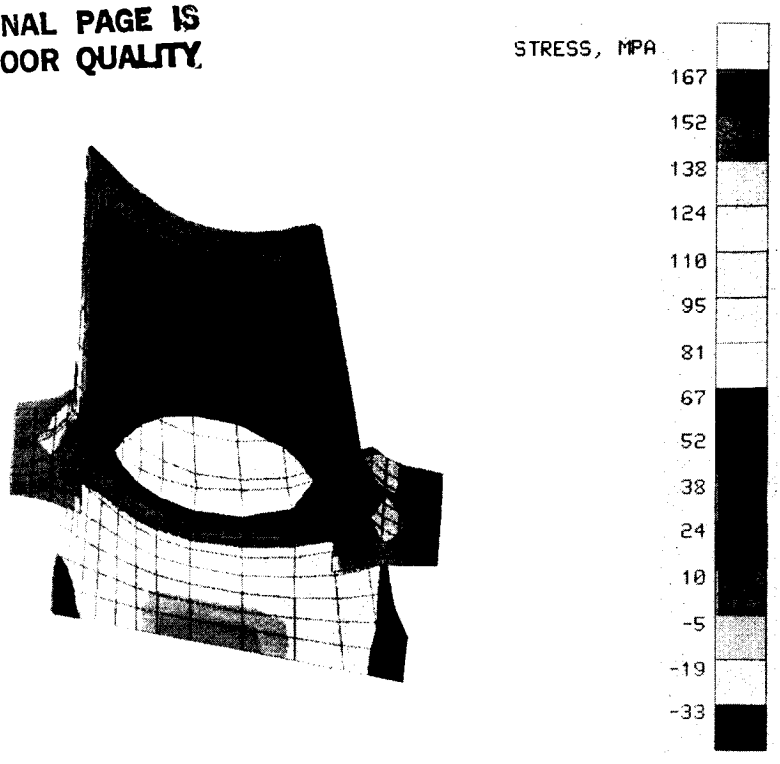

Figure 10. - Radial stresses at second ignition spike.

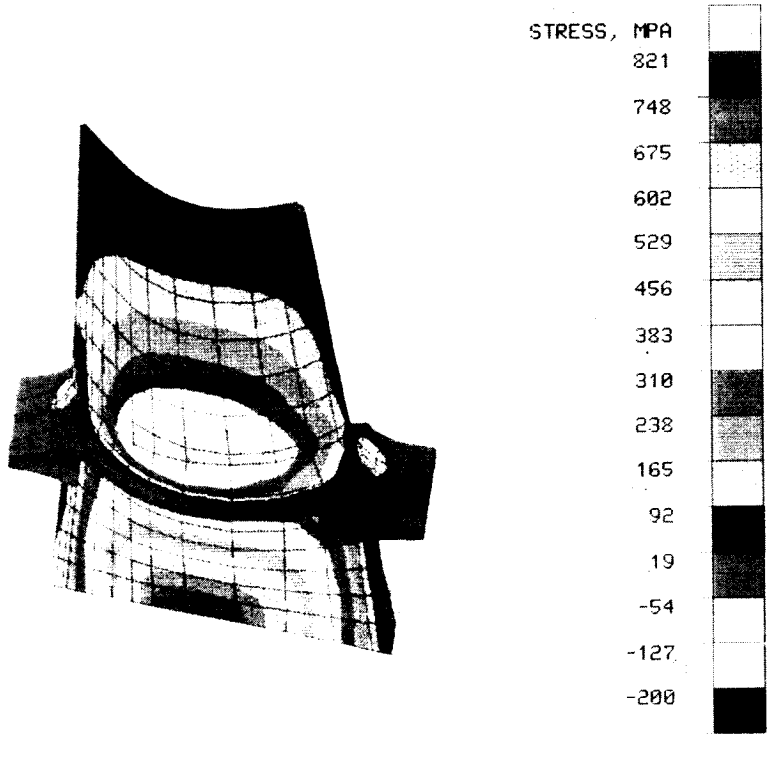

Figure 11. - Radial stresses during cruise.